American Mineralogist, Volume 88, pages 1138–1144, 2003

^{57}Fe Mössbauer-effect studies of Ca-rich, Fe-bearing clinopyroxenes: Part II. Magnetic spectra of magnesian hedenbergite

SIGRID G. EECKHOUT[1,2,*] AND EDDY DE GRAVE[1]

[1]Department of Subatomic and Radiation Physics, Ghent University, B-9000 Gent, Belgium
[2]Department of Geology and Soil Science, Ghent University, B-9000 Gent, Belgium

ABSTRACT

The magnetic properties of two natural magnesian hedenbergite samples with slightly different Fe contents (hereafter denoted HED1 and HED2) were studied by transmission ^{57}Fe Mössbauer spectroscopy within the temperature range 4.2–35 K and in a longitudinal, external field of 60 kOe at 4.2 K. The magnetic zero-field Mössbauer spectra (MS) were adequately refined using a superposition of two model-independent hyperfine-field distributions, one for the dominant Fe^{2+} component and one for the weak Fe^{3+} contribution, the positions of the eight absorptions and their intensities for each composing elemental subspectrum being determined by diagonalization of the hyperfine-interaction Hamiltonian. The maximum-probability saturation hyperfine fields for Fe^{2+} were found to be 180 kOe and 185 kOe for HED1 and HED2, respectively, while a value of ~545 kOe was obtained for Fe^{3+}. For both hedenbergite samples, the Fe^{2+} asymmetry parameter η of the electric field gradient (EFG) is quite high, namely 0.7–0.8 regardless of temperature. The orientation of the ferrous magnetic hyperfine field in the EFG principal-axes frame is ~(85°, 38°) and is not affected by the temperature of the absorber. The applied-field Mössbauer spectra show that the applied field does not disrupt the magnetic structure, and consequently that magnetic anisotropy is quite strong. The spectra were satisfactorily described by a two-parameter distribution model, taking into account distributions for the magnitude and the orientation of the hyperfine field with respect to the external field. The obtained hyperfine parameters are in excellent agreement with the results from the zero-field spectra. The temperature dependence of the hyperfine field seems to indicate that the magnetic structure in hedenbergite can be approximated by a two-dimensional rectangular Ising model and that the inter-chain and intra-chain magnetic exchange interactions are of similar magnitude.

INTRODUCTION

Hedenbergite, ideally $CaFe^{2+}Si_2O_6$, is a ferrous chain silicate belonging to the pyroxene group, which crystallizes in the monoclinic space group $C2/c$. The Fe^{2+}(M1) octahedra and Ca^{2+}(M2) polyhedra share edges to form laterally continuous sheets that lie parallel to the c axis. These sheets include zigzag chains of M1 sites sandwiched between two linear chains of M2 sites, and alternate with SiO_4 tetrahedral layers along asinβ (Cameron and Papike 1980). The linear chains of distorted M2 polyhedra are completely occupied by diamagnetic Ca^{2+} ions. Paramagnetic Fe^{2+} ions are located in the zigzag chains of more regular M1 octahedra, which are diluted by about 22% and 40% diamagnetic ions (mostly Mg^{2+}), in the two samples studied. In addition, a small amount of Fe^{3+} at the octahedral sites was observed (see Part I of these studies).

In the second part of this series of three papers on Ca-rich clinopyroxenes, the magnetic features of the hedenbergite samples HED1 and HED2 (see Part I) as reflected in their Mössbauer spectra (MS) recorded at $T < 30$ K and the interpretations of these MS are presented. A number of studies on the magnetic properties of hedenbergite have been reported in the past decades (e.g., Baum et al. 1997; Coey and Ghose 1985; Ghose et al. 1988; Hafner et al. 1999; Regnard and Boujida 1988; Tennant et al. 2000; Wiedenmann and Regnard 1986). It has been suggested that a ferromagnetic coupling exists between the Fe species within a particular M1 chain, and that the long-range magnetic ordering between neighboring M1 chains is antiferromagnetic. The positive paramagnetic Curie temperature shows that the ferromagnetic intra-chain interaction, which occurs via Fe-O-Fe superexchange, is stronger than the antiferromagnetic inter-chain interaction, the latter occurring via intervening SiO_4 groups (Baum et al. 1997; Coey and Ghose 1985; Regnard and Boujida 1988). Hafner et al. (1999) suggested that for strongly diluted samples (~40% Mg), the inter-chain, antiferromagnetic coupling might vanish.

On the basis of a literature review, some controversy exists concerning the Fe^{2+} spin direction. According to Ghose et al. (1988), the $C2/c$ space group allows for two different orientations of the spins, i.e., perpendicular or parallel to the b axis, which is the only (twofold) symmetry axis of the M1 site. On the basis of neutron diffraction analyses, Wiedenmann and Regnard (1986) concluded that the magnetic moments are lying in the a/c plane (i.e., perpendicular to the b axis), making an angle of 45° with the a axis. More recently, Baum et al. (1997) suggested from their magnetic susceptibility measurements on a natural single crystal, that the spins lie in the a/c plane, while Hafner et al. (1999) reported that the Fe^{2+} spin direction is in the ab plane, on the basis of magnetic susceptibility measurements.

* E-mail: sigrid.eeckhout@rug.ac.be

0003-004X/03/0007–1138$05.00

Coey and Ghose (1985) and Stanek et al. (1986) measured a magnetically split MS at 4.2 K for synthetic and natural hedenbergite, respectively. They obtained a hyperfine field, H_{hf}, of 188 kOe and 175 kOe, respectively. For natural magnesian hedenbergite with composition $Ca_{0.96}Fe_{0.82}Mg_{0.19}Mn_{0.02}Si_2O_6$ a discrete distribution of six hyperfine-field components, which were related to the possible Fe^{2+}-Mg^{2+} nearest-neighbor configurations surrounding the ^{57}Fe probe ion, was accounted for in order to describe the low-T MS (Regnard and Boujida 1988). Hafner et al. (1999) measured magnetically split MS for $CaFe_{1-x}Mg_xSi_2O_6$ (x = 0, 0.2, 0.3, 0.4, and 0.5) at 7 K. They observed for samples with $x > 0.2$ the coexistence of a paramagnetic and magnetic component, the latter showing a distribution of the hyperfine magnetic fields, which reflects, according to the authors, the coexistence of paramagnetic and ferromagnetic Fe clusters. According to Baum et al. (1988), the low-T ($6.5\ K \le T \le 15\ K$) MS for synthetic single crystals of the Fe^{3+} clinopyroxenes $LiFeSi_2O_6$ and $NaFeSi_2O_6$ exhibit relaxation effects, reflecting time fluctuations of the local magnetic fields. For $NaFeSi_2O_6$, a broadened, magnetic six-line pattern combined with a paramagnetic peak was observed at $6.5\ K < T \le 12.5\ K$. Baum et al. (1997) claim that also the MS for magnesian hedenbergite collected at 5 K exhibits relaxation phenomena. In contrast, De Grave et al. (1998) did not observe a coexistence of (super)paramagnetic and magnetic states for their aegirine sample and their analyses of the MS provide no indication that relaxation effects would be substantial. The authors ascribe the asymmetrically broadened sextet lines to chemical disorder.

In the present contribution the magnetic properties of the Fe^{2+}(M1) cations will be explored more profoundly and the temperature variation ($4.2\ K \le T \le 24\ K$) of the relevant hyperfine-field quantities will be discussed. The onset of magnetic ordering, determined by thermoscan measurements (see Part I of these studies), is 33 ± 1 K and 27 ± 1 K for HED1 and HED2, respectively. The application of an external magnetic field (4.2 K, 60 kOe) provides information on the nature of the magnetic ordering in hedenbergite. All details about the samples are presented in Part I and will not be repeated in the present paper.

Experimental methods

Transmission ^{57}Fe Mössbauer spectra (MS) were collected at temperatures between 4.2 and 35 K using conventional transmission Mössbauer spectrometers and standard cryogenic equipment (see Part I). The velocity range was ± 11 mm/s at 4.2 K and ± 7 mm/s at temperatures from 10 K to 30 K. The velocity scale was regularly calibrated with a α-Fe_2O_3 powder absorber or with a α-Fe foil at room temperature. All center-shift values quoted hereafter are referred to α-Fe. The absorbers (the same as those used in Part I) had a thickness of approximately 10 mg/cm^2 of natural Fe. The accumulation of data was continued until an off-resonance count of ~10^6 per channel was reached. At 4.2 K, MS were additionally collected in an external magnetic field of 60 kOe, applied parallel to the incident γ-ray beam.

Spectral analyses and results

Zero-field magnetic MS

The low-T MS (Fig. 1) are typical for Fe^{2+} ions in the magnetically ordered state, the strength of the quadrupole interaction being comparable to that of the magnetic-dipole interaction. In a first stage, the spectra for HED1 were refined on the basis of one single component and using the complete hyperfine-interaction Hamiltonian (HIH), which, by diagonalization, yields the energies and probabilities of the eight transitions from the ^{57}Fe nuclear ground states to the excited states, and hence the Mössbauer line shape. The adjustable hyperfine parameters were the center shift, δ, the quadrupole-coupling constant, $1/2e^2QV_{zz}$ or $6D$, the electric field gradient (EFG) asymmetry parameter, η, the hyperfine field, H_{hf}, and its orientation angles, ω and ψ (Fig. 2), and the line width, Γ. The experimental line shapes and intensities, however, were not adequately reproduced by the adjusted spectra using this procedure.

The broadening of the absorption lines ($\Gamma > 0.50$ mm/s) obviously suggests that a distribution of hyperfine fields might be present. Consequently, the spectra were fit (always using the HIH formalism) assuming a discrete distribution of six hyperfine-field components, as suggested by Regnard and Boujida (1988) for natural magnesian hedenbergite. The authors related

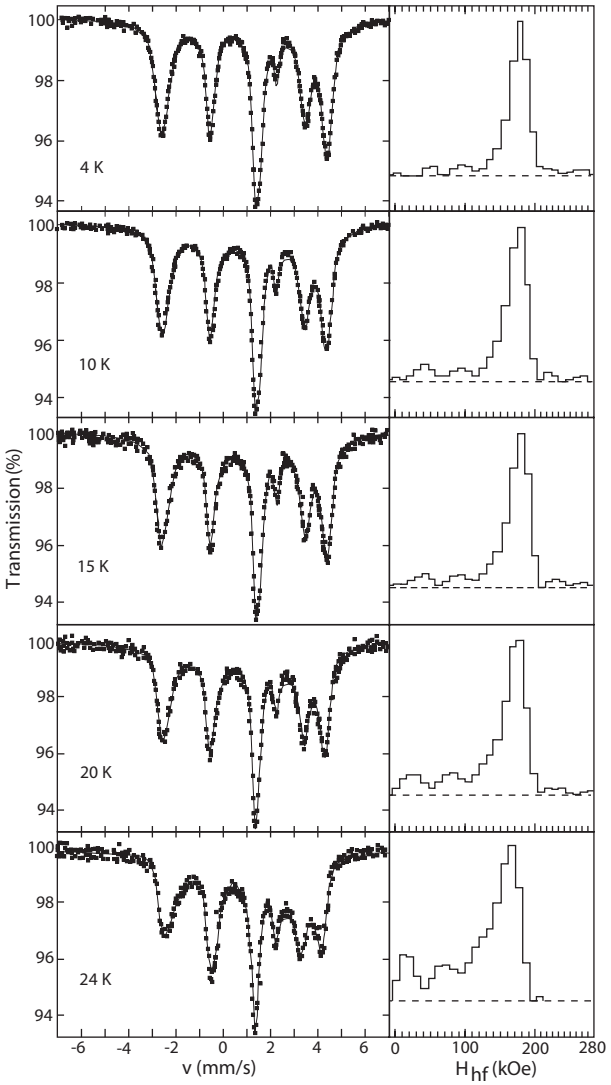

Figure 1. Experimental (squares) and calculated (solid lines) Mössbauer spectra and corresponding hyperfine-field, H_{hf}, distribution profiles at $T < T_N$ for HED1.

these distinct components to the different Fe^{2+}-Mg^{2+} nearest-neighbor (NN) and next-nearest neighbor (NNN) configurations to within the second cation shells surrounding the Fe^{2+} probe along the zigzag chains of M1 sites. Again, the line shapes and intensities could not be successfully described.

In a next stage, and comparable with the fitting procedure successfully applied to the paramagnetic MS of the same samples (see Part I), the low-T magnetic MS were calculated by a model-independent magnetic hyperfine-field distribution for Fe^{2+}. As before, the Fe^{2+} component was obtained from the complete HIH for each of the elemental Fe^{2+} components. The range for the hyperfine field, H_{hf}, was between 0 and 280 kOe and was varied in steps of 10 kOe. The adjustable parameters were the center shift, δ, the contribution of the z component of the EFG to the quadrupole splitting ($1/2e^2QVzz$ or $6D$), the asymmetry parameter, η, the angle between the EFG's principal axis and the direction of the hyperfine field, ω, the azimuthal angle of the hyperfine field in the principal-axes frame of the EFG, Ψ (Fig. 2), a linear correlation between $6D$ and H_{hf}, $C_{Q,hf}$, and between ω and H_{hf}, $C_{\omega,hf}$, and the line width, Γ, associated with the elemental nuclear transitions. The effect of ψ upon the calculated line shape is subordinate, and therefore a single value was considered for the fit. The correlations $C_{Q,hf}$ and $C_{\omega,hf}$ were introduced to optimize the intensities of the calculated absorptions. The physical background of the correlations is not obvious and would mean that the magnitudes of the various hyperfine interactions fluctuate in a correlated manner. This could be due to the chemical disorder around the probe nuclei, which affect these interactions.

The adjusted MS (solid lines), and the calculated H_{hf} distribution profiles for HED1 are reproduced in Figure 1. The agreement between the observed and fitted line shapes is excellent. The H_{hf} probability-distribution profile at 4.2 K is quite symmetric. The shallow maxima at the low and high hyperfine fields are believed to be artifacts of the fitting, rather than being indicative for the presence of distinct sites.

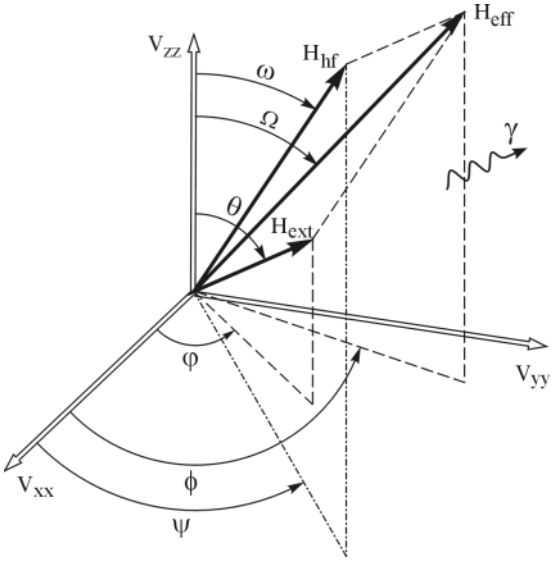

FIGURE 2. Vector addition of the applied field, H_{ext}, and internal field, H_{hf}, to the effective field, H_{eff}, with definition of the angles ω, θ, and Ω, and of the angles φ, Φ, and ψ with respect to the EFG's principal-axes frame.

Some numerical results of the one-dimensional H_{hf} distribution fitting procedure are listed in Table 1. The correlation coefficient $C_{\omega,hf}$ was found to be weak; on average, a change in field by 100 kOe is associated with a change of less than 1° in ω. For that reason, the $C_{\omega,hf}$ data are not included in Table 1 and a single ω value is considered. The correlation coefficient $C_{Q,hf}$ consistently decreases in magnitude with increasing T; the reason for this is unclear. The maximum-probability hyperfine field, H^m_{hf}, was found to be ~179 kOe at 4.2 K, which is within the range found earlier for both synthetic, i.e., 188 kOe (Coey and Ghose 1985) and natural, 170 kOe (Regnard and Boujida 1988; Stanek et al. 1986) hedenbergites, both quoted values referring to single-component fits. The polar angle ω (85° ± 5°) is in reasonable agreement with the value found by Coey and Ghose (1985), i.e., 74°. Hence, the direction of the field is close to perpendicular to the EFG's principal component, which likely lies along the c axis.

The asymmetry parameter η is quite high. Coey and Ghose (1985), Stanek et al. (1986), and Stanek (1987) reported values for η close to zero. No value for ψ is given in these papers; presumably it was assumed to be zero. The effect of ψ on the final line shape is indeed very small.

The field $H_{hf}{}^m$ gradually decreases with increasing temperature, while the orientation of the hyperfine field with respect to the EFG-axes frame remains unchanged. The values for δ, $\Delta E_Q{}^m$, and η are not affected by the temperature of the absorber and are furthermore in excellent agreement with those obtained from the low-temperature paramagnetic spectra (see Part I).

From the 4.2 K MS collected using a velocity range of ±11 mm/s (spectrum not shown) the appearance of a weak Fe^{3+} component is obvious. Its hyperfine field was found to be 547 ± 5 kOe, and its relative spectral area ~4%. In Part I the authors suggested the presence of a subordinate amount of octahedral ferric ions possibly attributable to the M1 sites, and the present magnetic MS tend to support that suggestion, at least to some extent because the magnetic Fe^{3+} subspectrum does not pro-

TABLE 1. Mössbauer results for the ferrous component in HED1 and HED2 at $T < T_N$

Sample	T	δ	$\Delta E_Q{}^m$	η	$H_{hf}{}^m$	ω^m	Ψ	$C_{Q,hf}$
HED1	4.2	1.31	2.57	0.71	180	81	39	–5.8
	10	1.31	2.57	0.78	177	84	39	–4.5
	15	1.32	2.59	0.74	178	82	39	–3.9
	20	1.32	2.56	0.78	175	85	38	–1.1
	24	1.32	2.55	0.78	167	84	38	0.0
HED2	8	1.31	2.62	0.77	185	84	38	–3.9
	15	1.32	2.60	0.77	182	84	38	–3.5
	20	1.32	2.53	0.78	177	87	37	–1.8
	25	1.31	2.61	0.81	161	90	37	–0.3
Error		0.01	0.04	0.15	2	3	8	1.0
Coey*	4.2	1.32	2.68	0.06	188	74	0	–
Regnard†	4.2	1.34	2.64	0.02	170	75	0	–

Notes: Temperature T (K), center shift δ (mm/s, relative to α-Fe at RT), quadrupole splitting ΔE_Q (mm/s), asymmetry parameter η, hyperfine field H_{hf} (kOe), the angle between the electric-field-gradient's (EFG) principal axis and the direction of the hyperfine field ω (°), the zenithal angle between EFG and the direction of the hyperfine field Ψ (°). The superscript m refers to the maximum-probability values. $C_{Q,hf}$ (10^{-3} mm/s.kOe) is the linear correlation coefficient between ΔE_Q and H_{hf}.

* Data from Coey and Ghose (1985).

† Data from Regnard and Boujida (1988).

vide any indication about the coordination type. As the middle and inner lines of the Fe^{3+} sextet are completely obscured by the Fe^{2+} absorptions, the other hyperfine parameters (center and quadrupole shifts) are ill defined and further identification of the ferric site cannot be concluded. As a consequence, no conclusions can be drawn concerning the ferric iron component.

The same procedure was used to describe the low-T MS for HED2. The results are given in Table 1. Within experimental error limits the HED2 results are identical to those obtained for HED1. This finding is not surprising since the two samples have very similar chemical compositions.

It is tempting to ascribe the distribution of hyperfine fields to the different Fe^{2+}-Mg^{2+} nearest-neighbor (NN) and next-nearest neighbor (NNN) configurations within the second cationic shell surrounding the Fe^{2+} probe along the zigzag chains of M1 sites, which is indeed reasonable thinking. However, Regnard and Boujida (1988) came to the conclusion that the approach of considering discrete spectral components, corresponding to the different cationic configurations and with probabilities as calculated from the well-known binomial law assuming a random distribution of the cations, is not supported by their observations. The present authors agree with this point of view. The probability profiles reproduced in Figures 1 and 2 do not exhibit any fine structure and hence provide no indication whatsoever that discrete hyperfine components are present or can be resolved. Rather, these profiles are indicative that quasi-continuous distributions of hyperfine fields govern the line shapes of the MS and in the authors' opinion, it is meaningless to try to relate quantitatively the evaluated H_{hf} probability profiles to the NN/NNN configurations alone. In general, such quantitative considerations are feasible and meaningful only when synthetic products are involved, for which the number of different cations is strictly limited and their amounts are well defined. In that case NNN effects may be quantified exactly as was recently demonstrated in a study of a series of synthetic enstatite–ferrosilite clinopyroxenes (Eeckhout et al. 2001).

It should be noted at this point that in a final stage of the data analysis, a two-parameter, model-independent approach was attempted. In this approach both the magnitude of the hyperfine field, H_{hf}, and its direction, ω, were allowed to vary between specified limits. For H_{hf} these limits were the same as in the previous one-parameter distribution fits. After numerous trial-and-error fits, a range for ω of 30–110°, with an increment of 5°, was eventually selected. The reproduction of the observed line shapes is adequate and the obtained χ^2 value is in general somewhat lower than for the one-parameter fits (but not substantially). The adjusted values of the relevant Mössbauer parameters are equal within experimental error limits to those of Table 1 (one-parameter fit). For all five applied temperatures, the maximum-probability angle, ω^m, is ~85° for both HED1 and HED2.

Applied-field magnetic MS (AFMS)

The AFMS recorded at 4.2 K for HED1 is shown in Figure 3. An obvious difference with respect to the zero-field MS is the clear appearance of shoulders outward the outer absorption lines. These shoulders appear at velocities ~–2.5 mm/s and ~4.4 mm/s, respectively, and coincide with the velocities of the outer

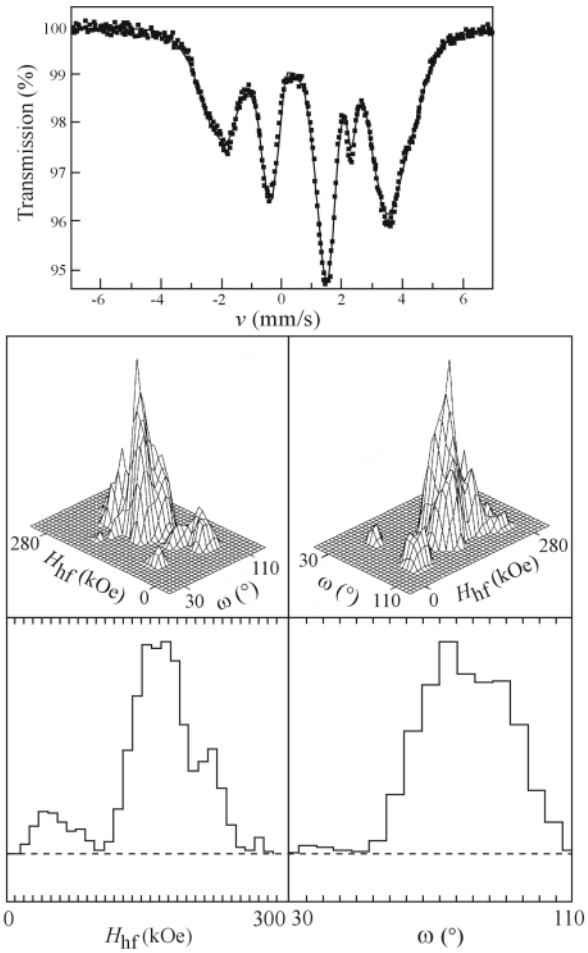

FIGURE 3. Experimental (squares) and calculated (solid lines) Mössbauer spectra obtained at 4.2 K in an external magnetic field of 60 kOe for HED1. The corresponding three-dimensional view of the (H_{hf}, ω) distribution, and the distribution of the integrated probabilities for ω and H_{hf} are depicted in the bottom drawings.

lines in the zero-field MS. The velocities of the more intense outer lines are shifted to lower magnitudes, i.e., ~–2 mm/s and 4.4 mm/s, respectively. At first glance, the origin of this feature is unclear, but, as will be demonstrated by the calculations presented in what follows, it is merely an effect of the applied external field. Apart from the appearance of the shoulders, the line shapes of the AFMS are very similar to those of the zero-field MS. This observation implies that the applied field does not disrupt the magnetic ordering pattern as reported in the literature (Baum et al. 1997; Coey and Ghose 1985; Regnard and Boujida 1988), and consequently that magnetic anisotropy is quite strong. Hafner et al. (1999) suggested that for moderately diluted hedenbergites, namely ~40% Mg, the antiferromagnetic coupling might vanish. In that case, a ferromagnetic ordering, or even a spin-glass-like ordering would be established. There is no indication, whatsoever, that such a breakdown effect occurs in the present samples.

When an absorber is subjected to an external magnetic field, $H_{ext,}$ the effective field, H_{eff}, experienced by the nucleus is the

vectorial addition of H_{ext} and H_{hf} (Fig. 2). When the absorber consists of a powder sample (as in the present case), presumably free of texture, the polar-angle set (θ, φ) is randomly distributed over the unit sphere. For each given set of (θ, φ) and knowing the magnitudes of H_{ext} and H_{hf}, the magnitude and direction of H_{eff}, i.e., the angles Ω and Φ, can be calculated in a straightforward manner using formulae of linear and spherical geometry. Their values can then be used in the HIH from which the Mössbauer line shape is calculated.

In the procedure programmed to fit the present AFMS, steps of 0.1 for cosθ in the range ±1 (i.e., θ varying from 90° to –90°) were considered, while φ was allowed to vary from 0° to 330° in increments of 30°. As for the zero-field MS, a model-independent distribution for H_{hf} was introduced, with the same upper and lower limits and with the same increments as used to analyze the zero-field MS. Also, a linear correlation coefficient, $C_{Q,hf}$, between $6D$ (or ΔE_Q) and H_{hf} was included, which was eventually found to be weak. In contrast to the results obtained for the zero-field MS, a significantly lower χ^2, and hence a more adequate reproduction of the observed line shape, was obtained if the angle ω had a distribution as well. After numerous trial-and-error fits, using the two-parameter distribution method (de Bakker et al. 1990), the interval (30°, 110°), in steps of 5°, was selected. Thus, in the final fitting approach ~120,000 spectral components had to be calculated from their respective HIH in each iteration step. However, the number of adjustable parameters was limited to six, i.e., δ, a ΔE_Q parameter and $C_{Q,hf}$, η, ψ, and a width parameter, Γ. For the sake of simplicity, the ferric component was neglected. Considering its low fractional contribution it would have been meaningless to include it in the fit.

The solid lines in Figure 3 represent the as such calculated line shapes. They adequately reproduce the observed MS. The adjusted relevant parameter values are listed in Table 2. They are in excellent agreement with the corresponding data indicated in Table 1 for the zero-field MS. Three-dimensional views of the (H_{hf}, ω) distributions, and the integrated distribution profiles for H_{hf} and ω are also depicted in the respective figures. They are very similar for the two hedenbergite species. The shapes of the (H_{hf}, ω) distributions may look odd. However, considering the complexity of the interplay between the various orientational factors affecting the AFMS, one can hardly expect to derive smoother distribution profiles from the observed line shapes.

The maximum-probability hyperfine field, $H_{hf,}^{m}$, was found to be 168 ± 5 kOe and 173 ± 5 kOe for HED1 and HED2, respectively. Both values are lower than those obtained from the zero-field MS (180 and 185 kOe respectively, Table 1). A similar effect was previously observed for the time-average $Fe^{2.5+}$ state in magnetite, while the hyperfine field for the Fe^{3+} species in the spinel structure was found to remain unaffected (De Grave et al. 1993). This lowering could imply that the external field induces an additional contribution to the hyperfine field or that it slightly affects the $3d$ wave functions of the probe Fe^{2+} cations.

TABLE 2. Mössbauer results for the ferrous component of HED1 and HED2 obtained at 4.2 K in an external field of 60 kOe

Sample	δ	ΔE_Q^m	η	H_{hf}^m	ω^m	Ψ
HED1	1.31	2.64	0.66	168	75	50
HED2	1.31	2.67	0.64	173	76	48
Error	0.01	0.04	0.15	2	3	8

Note: The symbols are the same as in Table 1.

Variations in the spectra with temperature

The variations with T of the center shifts and quadrupole splittings in the magnetically ordered regime were included in the interpretations of the $\delta(T)$ and $\Delta E_Q(T)$ curves discussed in Part I of this study.

The temperature dependencies of the Fe^{2+} hyperfine fields, H_{hf}, for HED1 and HED2 are depicted in Figure 4. Different theoretical models were used to interpret the $H_{hf}(T)$ curves. The three-dimensional mean-field or molecular-field model, leading to a Brillouin curvature (Morrish 1965), clearly failed, regardless of the value of the atomic spin S (2.0 or lower) used in the calculations. Subsequently, the hyperfine field was calculated in terms of the crystal-field model using data extracted from the $\Delta E_Q(T)$ curves.

Generally the hyperfine field consists of three main contributions: (1) the Fermi-contact term, H_F, which results from the unequal spin-up and spin-down (referred to the atomic spin) s-electron densities at the nucleus (Freeman and Watson 1965); (2) the orbital contribution, H_L, arising from the non-zero orbital momentum of the $3d$ electrons; and (3) the spin-dipolar term, H_{SD}, due to the spins of the electrons that have zero amplitude at the nuclear zone. In general, H_F is dominant, especially for Fe^{3+} for which H_L and H_{SD} are relatively small (order of ≤10 kOe, while $H_F \approx 500$ kOe). In contrast, for Fe^{2+} the three contributions may be of the same order of magnitude, however, with different signs.

The magnitude and sign of the total magnetic hyperfine field can be determined by calculation of the expectation values of the vector operators representing the three magnetic-interaction terms mentioned in the preceding paragraph. For that purpose, the complete crystal-field Hamiltonian (CFH), i.e., including spin-orbit coupling and spin-spin interaction, has to be diagonalized to obtain the $3d$ energy level scheme within the ^5D ground term. Similarly to the interpretation of the $\Delta E_Q(T)$ curves, the point-charge approach (see Part I) was used to construct the CFH. The Boltzmann populations of the resulting electronic levels subsequently allow the determination of H_{hf} at any given temperature below T_N. More details about these theoretical calculations are believed to be beyond the scope of this journal.

In the iterative fitting procedure, the value for the Fermi-contact term was in each step chosen such that the resulting saturation value for the hyperfine field was equal, within experimental error, to the hyperfine field obtained from the MS recorded at 4.2 K. The values for $|H_F|$, $|H_L|$, and $|H_{SD}|$ corresponding to these theoretical T variations are 305, 380, and 105 kOe for both hedenbergite species, with H_L and H_{SD} having the sign (positive) opposite to that of H_F. The magnitude of the orbital contribution is rather high and confirms the (qualitative) suggestion of Regnard and Boujida (1988). The reproduction of the experimental $H_{hf}(T)$ data, however, seems to be inadequate (curves marked "p" in Fig. 4). One must consider,

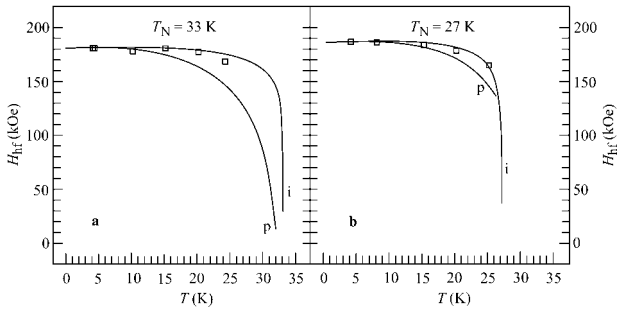

FIGURE 4. Experimental (open boxes) and calculated (solid lines) temperature dependence of the hyperfine fields $H_{hf}(T)$ using the point-charge approach (p curves) and using the two-dimensional rectangular Ising model (i curves) for HED1 (**a**) and HED2 (**b**).

however, that the number of experimental data points in the crucial temperature region, i.e., between ~20 K and T_N, is very limited (actually only two points are available).

The approach summarized above allows us to predict the orientation of H_{hf} in the EFG principal-axes frame, and hence with respect to the crystallographic axes. According to Ghose et al. (1988), the $C2/c$ space group allows for two different orientations of the spins, i.e., perpendicular or parallel to the b axis, which is the only (twofold) symmetry axis of the M1 site. The point-charge model used here leads to a parallel orientation for both the hyperfine field and the magnetic moment. However, this result seems to be in disagreement with neutron diffraction analyses that infer that the magnetic moments are lying in the *ac* plane (Coey and Ghose 1985; Wiedenmann and Regnard 1986; Ghose et al. 1988). Also Baum et al. (1997) concluded that the spins lie in the *ac* plane on the basis of their susceptibility measurements on a natural single crystal of magnesian hedenbergite with an iron content of 0.84 apfu. In contrast, Hafner et al. (1999) quoted that the Fe^{2+} spin direction is in the *ab* plane. Obviously, this statement is based on a misinterpretation since the authors refer to the paper of Wiedenmann and Regnard (1986).

In spite of these disagreements concerning the field direction, the point-charge model correctly predicts the magnitude of the magnetic moment. For both hedenbergites the calculated orbital and spin magnetic moments are $\langle L \rangle \approx 0.74\ \mu_B$ and $\langle S \rangle \approx 1.97\ \mu_B$, respectively. Assuming the same covalence-reduction factor α (see Part I) for both moments, the total moment is $\alpha \langle L + 2S \rangle \approx 4.3\ \mu_B$, which is in excellent agreement with the reported values, namely 4.2 μ_B (Wiedenmann and Regnard 1986) and 4.94 μ_B (Baum et al. 1997) for natural and 4.33 μ_B (Ghose et al. 1988) for synthetic hedenbergite.

Several authors have considered the magnetic ordering in hedenbergite as one-dimensional (Ghose et al. 1988; Regnard and Boujida 1988; Wiedenmann and Regnard 1986; Hafner et al. 1999). This idea emanated from the presumed strong ferromagnetic coupling between the spins within a particular M1 chain, and the presumed much weaker antiferromagnetic coupling between two adjacent M1 chains. However, Kramers and Wannier (1941) have convincingly shown that such linear chains of spins cannot order ferromagnetically and that, hence, no magnetic hyperfine field is present. Consequently, a quasi one-dimensional approximation for the magnetic structure in hedenbergite is not justified.

The zigzag chains of M1 sites can be considered as two interacting linear chains within the same plane. Two magnetic intraction paths are important, namely the so-called vertical one (the ferromagnetic intra-chain exchange, J_1) along the chain axis, and the horizontal interaction (the antiferromagnetic inter-chain exchange, J_2) between two M1 chains, which are bridged via the tetrahedral chain. Considering the rather large Fe-Fe distance between Fe species in neighboring M1 chains, namely 5.711 Å (Baum et al. 1997), one would expect that the antiferromagnetic interaction between two such chains plays a minor role. Since it may be expected that $J_1 \neq J_2$, this structure may be regarded as a rectangular type of two-dimensional magnetic ordering (Chang 1952). According to this author, in the two-dimensional rectangular Ising model the temperature variation of the reduced magnetization m_S can be expressed as:

$$m_S = \left[1 - \left(\frac{2x_1}{1-x_1^2} \cdot \frac{2x_2}{1-x_2^2}\right)^2\right]^{1/8} \quad (1)$$

in which $x_i = \exp\left(-\frac{J_i}{kT}\right)$ with $i = 1, 2$. Since the spontaneous magnetization disappears at $T = T_N$, the following equation is valid at that temperature:

$$(x_1 + 1)\,(x_2 + 2) = 2 \quad (2)$$

This latter condition means that the ratio J_1/J_2 of the interaction strengths determines the ordering temperature. In the critical temperature interval $0.9\ T_N < T < T_N$ the reduced spontaneous magnetization varies as (Chang 1952)

$$m_s(T) \cong \left(1 - \frac{T}{T_N}\right)^{1/8} \quad (3)$$

The exponent 1/8 depends only upon the magnetic dimensionality of the lattice and not upon the ratio $\frac{J_1}{J_2}$ or upon the number of magnetic neighbors.

To a first approximation, the hyperfine field in general is proportional to the spontaneous magnetization, and Equation 1 can therefore be used to formulate the temperature variation of the hyperfine field, $H_{hf}(T)$, as:

$$H_{hf}(T) = H_{hf}(0\ \mathrm{K})\left[1 - \left(\frac{2x_1}{1-x_1^2} \cdot \frac{2x_2}{1-x_2^2}\right)^2\right]^{1/8} \quad (4)$$

Since for both hedenbergite species the values for T_N are known (see Part I) and since the $H_{hf}(T)$ curves are experimentally determined, and assuming further that $H_{hf}(0\ \mathrm{K})$ equals the hyperfine-field value measured at 4.2 K, J_1 (or J_2) can be determined by adjusting Equation 3 to the experimental results. This approach was successfully applied to HED1 and HED2. The adjusted $H_{hf}(T)$ curves are reproduced in Figure 4, labeled "i", and apparently provide a satisfactory description of the observed temperature variations. For both hedenbergite species, the magnitudes of the exchange integrals J_1 and J_2 were found to be 30 K and 24 K, respectively, with an estimated error of 5 K. This error is relatively high, but considering the small number of observations, it is believed not to be overestimated. In conclusion, the present results seem to confirm that the magnetic struc-

ture in hedenbergite can be approximated by a two-dimensional rectangular Ising model, and that the inter-chain and intra-chain magnetic exchange interactions are of similar magnitude.

ACKNOWLEDGMENTS

The authors thank A. Van Alboom for his assistance in programming the computer routines and in carrying out and interpreting the results of the model calculations. They are much indebted to the Fund for Scientific Research–Flanders for the financial support that enabled to carry out the numerous experiments involved in this study.

REFERENCES CITED

Baum, E., Treutmann, Z., Behruzi, M., Lottermoser, W., and Amthauer, G. (1988) Structural and magnetic properties of the clinopyroxenes $NaFeSi_2O_6$ and $LiFeSi_2O_6$. Zeitschrift für Kristallographie, 183, 273–284.

Baum, E., Treutmann, W., Lottermoser, W., and Amthauer, G. (1997) Magnetic properties of the clinopyroxenes aegirine and hedenbergite: a magnetic susceptibility study on single crystals. Physics and Chemistry of Minerals, 24, 294–300.

Cameron, M. and Papike, J.J. (1980) Crystal chemistry of silicate pyroxenes. In C.T. Prewitt, Ed., Pyroxenes, p. 1–92. Reviews in Mineralogy, Mineralogical Society of America, Washington, D.C.

Chang, C.H. (1952) The spontaneous magnetization of a two-dimensional rectangular Ising model. Physical Review, 88, 1422.

Coey, J.M.D. and Ghose, S. (1985) Magnetic order in hedenbergite: $CaFeSi_2O_6$, Solid State Communications, 53, 143–145.

de Bakker, P.M.A., De Grave, E., Persoons, R.M., Bowen, L.H., and Vandenberghe, R.E. (1990) An improved, two-parameter distribution method for the description of the Mössbauer spectra of magnetic small particles in an applied field. Measurement Science and Technology, 1, 954–964.

De Grave, E., Persoons, R.M., Vandenberghe, R.E., and de Bakker, P.M.A. (1993) Mössbauer study of the high-temperature phase of Co-substituted magnetites, $Co_xFe_{3-x}O_4$. I. $x \leq 0.04$. Physical Review B, 47, 5881–5893.

De Grave, E., Van Alboom, A., and Eeckhout, S.G. (1998) Electronic and magnetic properties of a natural aegirine as observed from its Mössbauer spectra. Physics and Chemistry of Minerals, 25, 378–388.

Eeckhout, S.G., De Grave, E., Lougaer, A., Gerdan, M., McCammon, C.A., Trautwein, A.X., and Vochten, R. (2001) Magnetic properties of synthetic $P2_1/c$ Mg-Fe clinopyroxenes as observed from their low-temperature Mössbauer spectra and from SQUID magnetization measurements. American Mineralogist, 86, 957–964.

Freeman, A.J. and Watson, R.E. (1965) Hyperfine interactions in magnetic materials. In G.T. Rado, and H. Suhl, Eds., Magnetism IIA, p. 167–305. Academic Press, New York.

Ghose, S., Hewat, A.W., Van Dang, N., and Weidner, J.R. (1988) Magnetic phase transitions in quasi-one dimensional antiferromagnets: ferrosilite, $Fe_2Si_2O_6$, and hedenbergite, $CaFeSi_2O_6$. Materials Science Forum, 27/28, 235–242.

Hafner, S.S., Stanek, J., and Treutmann, W. (1999) One-dimensional ferromagnetic chains in $CaFe_{1-x}Mg_xSi_2O_6$. Proceedings XXXIV Zakopane School, 179–184.

Kramers, H.A. and Wannier, G.H. (1941) Statistics of the two-dimensional ferromagnet. Part I. Physical Review, 60, 252–263.

Morrish, A.H. (1965) The physical principles of magnetism. 680 p. Wiley, New York.

Regnard, J.R. and Boujida, M. (1988) Relations between magnetic hyperfine field distribution and cation order in natural hedenbergite. Hyperfine Interactions, 41, 513–516.

Stanek, J. (1987) Temperature dependent asymmetry parameter of the electric field gradient on $^{57}Fe^{2+}$. Nuclear Instruments and Methods in Physics Research B, 22, 577–580.

Stanek, J., Hafner, S.S., Regnard, J.R., and El Goresy, J. (1986) Temperature-dependent hyperfine parameters in $CaFeSi_2O_6$. Hyperfine Interactions, 28, 829–832.

Tennant, W.C., McCammon, C.A., and Miletich, R. (2000) Electric-field gradient and mean-squared-displacement tensors in hedenbergite from single-crystal Mössbauer milliprobe measurements. Physics and Chemistry of Minerals, 27, 156–163.

Wiedenmann, A. and Regnard, J.R. (1986) Neutron diffraction study of the magnetic ordering in pyroxenes $Fe_xM_{1-x}SiO_3$, Solid State Communications, 57, 499–504.

MANUSCRIPT RECEIVED APRIL 2, 2002
MANUSCRIPT ACCEPTED NOVEMBER 15, 2002
MANUSCRIPT HANDLED BY DARBY DYAR